Optimization Design of Heliostat Field Based on Genetic Algorithm with Traversal Strategy

Xiao Liu [1, *, #], Jinxian Dong [2, #], Siying Wang [1, #]

[1] School of Automation, Jiangsu University of Science and Technology, Zhenjiang, China, 212100

[2] School of Economics and Management, Jiangsu University of Science and Technology, Zhenjiang, China, 212100

* Corresponding Author Email: lx15753869905@163.com

[#]These authors contributed equally.

Abstract. This study aims to analyze the average efficiency and thermal power output of a heliostat field. A horizontal coordinate system and a mirror coordinate system are established with the center of the mirror field and the center of each heliostat as the origins, respectively. The study considers various factors including three types of shadowing and blockage scenarios, and spillage efficiency. Using rotation matrices and linear equations, a shadowing and blocking efficiency model is constructed. Combining the principles of concentration, ray tracing method, and geometric theory, the energy flux density is converted into a number of scatter points, and then a model for the various efficiencies and thermal power output of the heliostat field is established. Based on this, an optimization model is created with the objective of maximizing the average annual thermal power output per unit mirror area. A genetic algorithm based on a traversal strategy is used for solving this model, thereby facilitating the design of the parameters for the heliostats and the receiver tower in the heliostat field, improving the average annual thermal power output per unit mirror area, and providing assistance for theoretical research.

Keywords: Optical Efficiency, Ray Tracing Method, Mirror Field Layout. Genetic Algorithm.

1. Introduction

With the development of the economy and society, and the proposal of China's green and sustainable development goals, the pollution-free utilization of solar energy as a renewable energy source has become an important topic in China's energy sector. Tower-type solar thermal power generation is an emerging low-carbon and environmentally friendly clean energy technology. By researching certain parameters in the heliostat field, it is possible to maximize the average annual thermal power output per unit mirror area. This contributes to improving the efficiency of tower-type solar power generation and holds significant importance for China in achieving its 'carbon peak' and 'carbon neutrality' goals.In this paper, we will study the following issues:

(1)Assuming that a receiver tower is installed at the center of a circular heliostat field, with each heliostat measuring 6m×6m and mounted at a height of 4m, and knowing the positions of all heliostat centers, the absorption tower is located at the center of the circular heliostat field, and there are no heliostats distributed within a 100m radius around the absorption tower, calculate the annual average optical efficiency, annual average thermal power output, and annual average thermal power output per unit mirror area of this heliostat field.

(2) Assuming that all heliostats are of the same size and have the same installation height, design the parameters of the heliostat field: the position coordinates of the absorption tower, the size of the heliostats, the installation height, the number, and the positions of the heliostats, in order to enable the heliostat field to achieve the designated annual average output thermal power.

2. Research Method

Establish a horizontal coordinate system with the absorption tower as the origin and determine the position of the sun through the solar declination angle, altitude angle, azimuth angle, and hour angle.

Consider the shadow occlusion losses between adjacent heliostats and from the absorption tower to the heliostats during incidence and reflection. Establish a mirror coordinate system and use the rotation matrix equation and the point-to-vector equation to calculate the ground projection of the vertex and the covered area, thereby establishing a shadow occlusion efficiency model. Determine the unit vectors of incident and reflected light based on the heliostat concentration principle to obtain the cosine efficiency model. Use ray tracing to convert energy into the number of scatters points and establish an interception efficiency model through geometric and coordinate transformations. Finally, establish an atmospheric transmittance model. Solve the model to obtain the annual average optical efficiency of the heliostat field, the annual average output thermal power, and the annual average output thermal power per unit mirror area.

Building upon the previous model, this approach establishes a single-objective optimization model with the coordinates of the absorption tower, the length of the heliostat, the width of the heliostat, and the installation height as decision variables. The goal is to maximize the annual average output power per unit mirror area. This model takes into consideration various constraints including the radius of the heliostat, boundary constraints of the heliostat, size constraints of the heliostat, height constraints of the heliostat, power constraints, and spacing constraints between heliostats. Using genetic algorithms, the optimal parameters for the absorption tower are determined.

3. Establishment of the Heliostat Field Efficiency and Output Thermal Power Model

3.1. Determination of the Sun's Position

Taking the center of the circular heliostat field as the origin, with the eastward direction as the x-axis and the northward direction as the y-axis, and the direction perpendicular to the ground and upward as the positive z-axis, a horizontal coordinate system is established. The position of the sun is determined using the solar altitude angle and the solar azimuth angle, as shown in Figure 1.

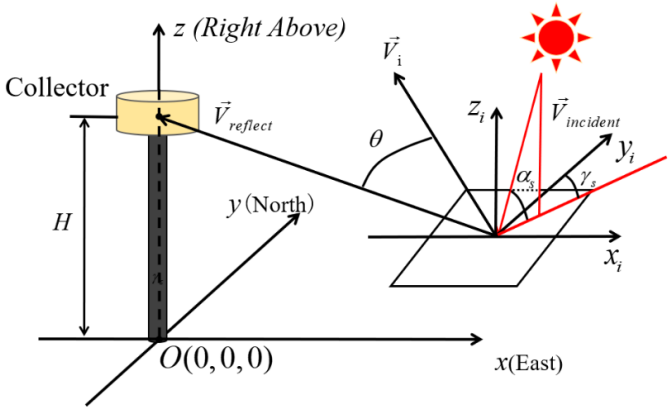


Figure 1. Schematic Diagram of Horizontal Coordinate System and Heliostat Concentration

According to the literature [1], the solar altitude angle (α_s) and azimuth angle (γ_s) can be determined based on the local latitude(φ), the solar declination angle(δ), and the solar hour angle(ω), thereby determining the position of the sun:

$$\begin{cases} \sin\delta = \sin\frac{2\pi D}{365}\sin(\frac{2\pi}{360}23.45) \\ \omega = \frac{\pi}{12}(ST-12) \\ \sin\alpha_s = \cos\delta\cos\varphi\cos\omega + \sin\delta\sin\varphi \\ \cos\gamma_s = \frac{\sin\delta - \sin\alpha_s\sin\varphi}{\cos\alpha_s\cos\varphi} \end{cases} \quad (1)$$

Wherein: D is the number of days counted from the spring equinox, with the day of the spring equinox being March 21st; ST is the local time; φ is the local latitude, with northern latitude being positive.

3.2. The determination of the shadow blocking efficiency model

The heliostat field is located north of the Tropic of Cancer 23.5°, at east longitude 98.5° and north latitude 39.4°, thus the sun moves from east to west on the south side of the mirror field. At this time, the shadow blocking loss mainly includes two parts: the shadow loss $S_{sb-tower}$ of the absorption tower during incidence; and the mirror surface shadow and blocking loss S_{sbi} during incidence and reflection.

As shown in Figure 2, the projection of the absorption tower can be determined by special points A, B, and C. When the projection of the absorption tower on the ground intersects with the projection of the heliostat on the ground, the heliostat is obscured by the absorption tower.

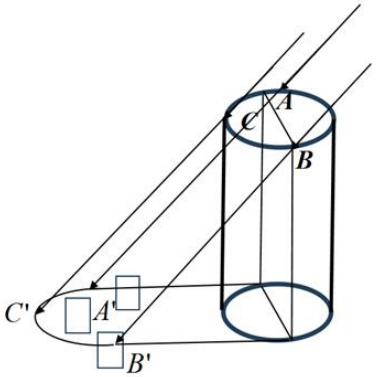


Figure 2. Absorption Tower Shadow Loss Diagram

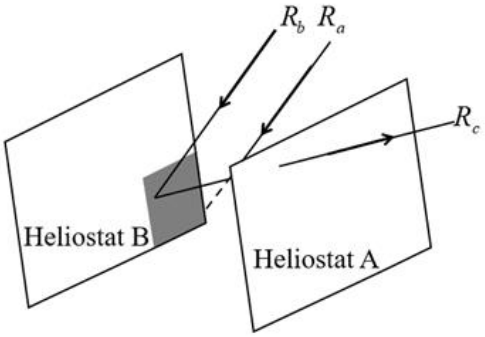


Figure 3. Heliostat Obstruction Loss Diagram

As shown in Figure 3, R_a and R_b represent the incident sunlight, and R_c represents the reflected light. The heliostat closest to and facing the sun from mirror B is denoted as mirror A. As can be understood from the path of the light rays, the incident ray R_a is blocked by mirror A in the process of reaching mirror B, causing a shadow of mirror A on mirror B. The reflected ray R_c is obstructed by mirror B in the process of reaching the collector, resulting in mirror A causing an obstruction phenomenon on mirror B.

The light rays pass through special points A, B, and C and are projected onto the ground plane. Similarly, the shadow area is calculated by finding all the edge points. The shadow occlusion loss τ_{sb} can be represented as follows:

$$\tau_{sb} = (S_{sbi} \bigcup S_{sb-tower}) / \sum_{i=1}^{N} A_i \tag{2}$$

Where: A_i represents the area of the reflective surface, and N is the total number of reflective surfaces.The final Shadow Obstruction Efficiency η_{sb} [2] can be obtained as follows $\eta_{\mathrm{sb}} = 1 - \tau_{sb}$.

3.3. Determination of the Cosine Efficiency Model

As shown in Figure 1, when reflecting sunlight onto an absorber, there is inevitably an angle θ between the incident solar rays and the normal to the heliostat mirror surface.When the direction of the incident sunlight is not parallel to the normal of the mirror surface, it causes a loss of received energy. In this case, the cosine loss is $\tau_{\cos}$, and the cosine efficiency $\eta_{\cos}$ [3] can be expressed as:

$$\eta_{\cos} = 1 - \tau_{\cos} = \cos\theta = \left| \frac{1+\cos(2\theta)}{2} \right| = \left| \sqrt{\frac{1-\vec{V}_{\text{incident}} \cdot \vec{V}_{reflect}}{2}} \right| \tag{3}$$

3.4. Determination of the Blocking Efficiency Model

The ray tracing method [4] is used to track the position where any one of the solar rays, after being reflected by the heliostat, falls on the collector. With the center of the light cone's cross-section as the origin O_{cone} and the half-angle spread direction as the x_{cone}-axis, a light cone coordinate system is established, as shown in the following figure:

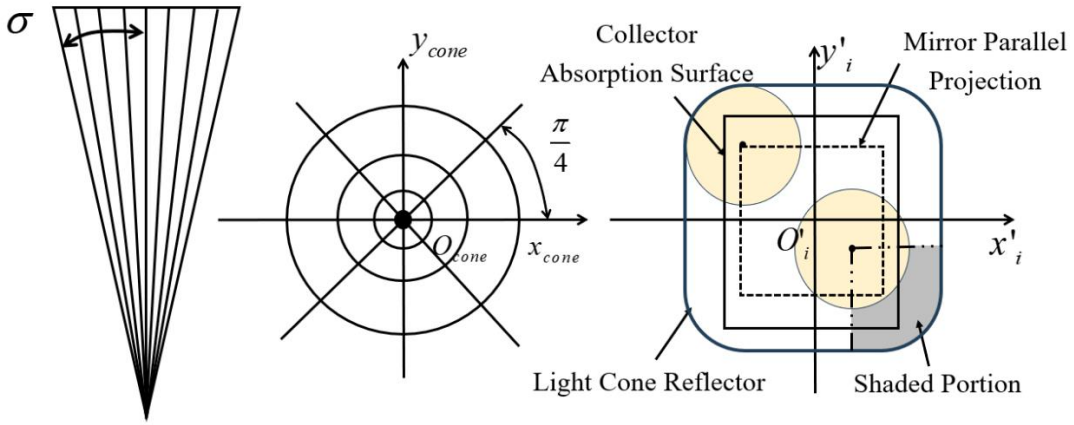


Figure 4. Schematic Diagram of Energy Absorption by Angle Division Method and Scatter Method

Establish a coordinate system with the center of the light cone imaging surface as the origin (as shown in Figure 4), where the coordinates of point A on the light cone section in the light cone imaging surface coordinate system can be represented as $(x_p + x_{pcone}, y_p + y_{pcone})$. Considering the scattering of the light cone, the imaging surface of the light rays is slightly larger than the plane of the collector. The reflective mirror surface is divided into n regions, each corresponding to a vertex (x_p, y_p) of a light cone. The vertices of the light cone that fall on the shaded part of the mirror, which blocks light, do not produce energy on the collector and have no corresponding light cone scatter points. The coordinates of the points on the light cone section coordinate system are (x_{cone}, y_{cone}).

Remember that the pitch Angle of the reflected light is α_{reflet}.Take the two parallel planes of vertically reflected light as shown in Figure 5. θ_1 is the Angle between the mirror and the vertical reflected light plane, that is, the Angle between the normal vector of the mirror and the reflected light; θ_2 is the Angle between the reflected light and the z axis, namely $\pi/2 - \alpha_{reflet}$.

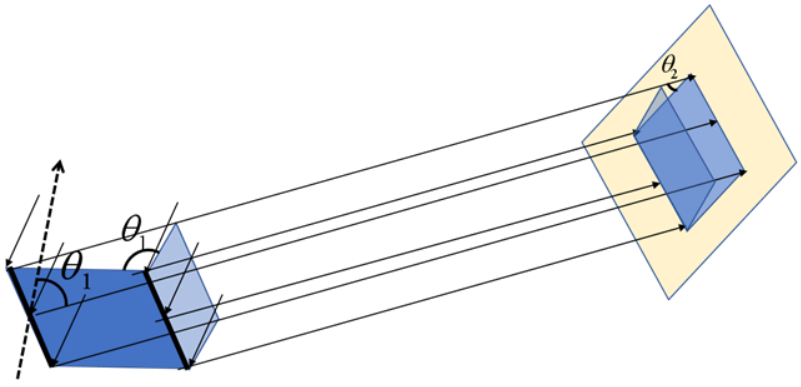


Figure 5. Mirror Imaging on the Collector Receiver Surface

After converting the mirror to the collector plane, the width change of the mirror is small and can be ignored,and the center of the mirror after conversion coincides with the collector plane. The difference between mirror total reflection energy $e_{reflect}$ and shadow occlusion lost energy e_{cover} is the number of all existing points on the collector coordinate system, and the collector received energy $e_{receive}$ is the number of points falling within the range of the collector, thus the collector truncation efficiency η_{trunc} [5-6]:

$$\eta_{\text{trunc}} = \frac{e_{receive}}{e_{reflect} - e_{cover}} \tag{4}$$

3.5. Determination of the Atmospheric Transmittance Model

As sunlight propagates through the air, its rays are affected by dust, particles, and other elements in the air, causing a certain degree of attenuation. Therefore, in the path of light reflection from the mirror surface to the absorber, the extent of loss varies slightly depending on the distance between the mirror surface and the reflection target point.

$$\eta_{\text{at}} = 0.99321 - 0.0001176 d_{HR} + 1.97 \times 10^{-8} \times d_{HR}^2 \tag{5}$$

Where: d_{HR} is the distance from the center of the mirror to the center of the collector, $d_{HR} \le 1000$. Based on the known coordinates of the center of each reflector's base from previous data, this is calculated using the distance formula between two points.

3.6. Determination of the Heliostat Optical Efficiency and Output Thermal Power Model

The optical efficiency (η) of the heliostat can be obtained as:

$$\eta = \eta_{\text{sb}} \eta_{\cos} \eta_{\text{at}} \eta_{\text{trunc}} \eta_{\text{ref}} \tag{6}$$

Where, η_{ref} is mirror reflectivity and the constant is 0.92.

By consulting the data, the normal direct radiation illuminance DNI [7-8] can be calculated, from which the output thermal power E_{field} of the heliostat field can be expressed as:

$$E_{\text{field}} = \text{DNI} \cdot \sum_{i=1}^{N} A_i \eta_i \tag{7}$$

Where: η_i is the optical efficiency of the i mirror.

It can be obtained that the annual average optical efficiency, annual average thermal output power and annual average output power per unit mirror area of the heliostat field can be expressed as:

$$\begin{aligned} \overline{\eta} &= \sum_{month}^{12} \sum_{hour}^{5} \sum_{i=1}^{N} \eta_i \\ \overline{E_{field}} &= \left(\sum_{month}^{12} \sum_{hour}^{5} E_{field} \right) / 60 \\ \overline{E_i} &= \sum_{month}^{12} \sum_{hour}^{5} \frac{E_{\text{field}}}{N \cdot A_i} \end{aligned} \tag{8}$$

3.7. The solution for the efficiency of the fixed sun mirror field and the output thermal power

In this context, the requirement for shadow occlusion efficiency implies a demand for shadow occlusion loss. The shadow occlusion loss is determined by the area $S_{sb-tower}$ of the shadow occluded

by the absorption tower and the area of shadow occlusion during incidence and reflection. The mirror coordinate system is established as shown in Figure 6.

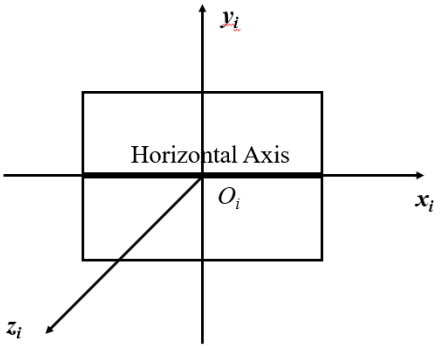


Figure 6. Mirror coordinate system

By using a rotating coordinate system [9], the coordinates of the heliostat vertex in the horizontal coordinate system and its ground projection coordinates are solved, thereby obtaining the projection area S'_{mirror} of the heliostat vertex on the ground. The overlapping area $S'_A \cap S'_B$ between Mirror A and Mirror B is calculated. The shadow area $S'_{sb-incident} = S'_A \cap S'_B$ overlapping on Mirror B in the incident coordinate system is recorded. Similarly, the occlusion area $S'_{sb-reflect} = S'_{A'} \cap S'_{B'}$ during reflection is obtained. Thus, the shadow occlusion area S'_{sbi} generated between the mirrors on the ground is determined.

$$S'_{sbi} = S'_{sb-incident} \cup S'_{sb-reflect} = (S'_A \cap S'_B) \cup (S'_{A'} \cap S'_{B'}) \tag{9}$$

Similarly, when the tower projection area overlaps with the mirror projection area, it is considered to be affected by the tower's occlusion; otherwise, it is not affected. Hence, the shadow area on the ground projection surface caused by the tower is obtained.

Since the projection of the light direction on the ground forms a parallelogram, and knowing the dimensions of the heliostat are 6m × 6m, the occluded area on the ground is converted into the shadow area S_{sbi}, $S_{sb-tower}$ on the heliostat based on the ratio (the shadow area to the total area of the heliostat).

Solve the model to obtain the average efficiencies for each 21st day of the month, as well as the annual average thermal power output per unit mirror area. The average optical efficiency on the 21st of each month and the average output thermal power per unit mirror surface area continuously change over time, showing a trend of first increasing and then decreasing, with the maximum output thermal power occurring on the summer solstice.

The annual average optical efficiency and output power are as shown in Table 1.

Table.1. The annual average optical efficiency and output power

annual average optical efficiency	annual average cosine efficiency	Average annual shadows Sheltering efficiency	annual average truncation efficiency	Average annual output Thermal power (MW)	Annual average of mirrors per unit area Output thermal power (KW/m)2
0.5888	0.7565	0.8999	0.9536	35.9517	0.5723

According to the data in the table, the annual average shadow occlusion efficiency is high, indicating significant power loss. This suggests that there is still room for improvement in the fixed sun mirror field.

4. Optimization modeling of the fixed-heaven mirror field

Decision variables: Establish an optimization model by taking the coordinates of the absorption tower, the length of the heliostat, the width of the heliostat, and the installation height as four decision variables, so as to optimize the design of the heliostat field.

Objective Function: An objective function is established with the goal of maximizing the annual average power output per unit mirror area:

$$\max \frac{\sum_{month}^{12}\sum_{hour}^{5} E_{\text{field}}}{\sum_{i=1}^{N} A_i} \tag{10}$$

Where: $month$ is the month and $month = 1, 2, \cdots, 12$ corresponds to the 21st day of the 12th month; $hour$ is the time and $hour = 1, 2, \cdots, 5$ corresponds to 9:00, 10:30, 12:00, 13:30 and 15:00 respectively.

Constraints: In the process of arranging the heliostats, it is necessary to consider the safe spacing between the heliostats, and then minimize the shadow blocking temperature problem between the heliostats while increasing the utilization rate of the circular heliostat field.

Considering the contradiction between the land utilization rate of the heliostat field and the shadow shading of the heliostat mirrors, the mirrors are distributed in eccentric circles around the absorption tower, and the annual average output power per unit mirror area is the largest, and the radial spacing of the heliostat mirrors can be obtained according to the mirror field transmission efficiency threshold and the projection method, as shown in Figure 7:

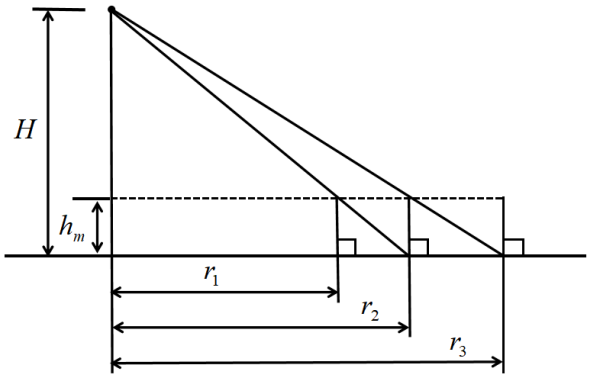


Figure 7. Schematic of heliostat spacing

Constraint 1: According to the calculation method of the mirror field boundary can determine the distance between the first row of heliostats and the absorption tower, according to the geometrical relationship can be found in the expression of the distance between the heliostats and the collector tower, there is a radius constraint of the heliostat:

$$r_q = r_1 h_{tower}{}^{q-1} / (h_{tower} - h_m)^{q-1} \tag{11}$$

Where: r_q is the distance between the qth ring heliostat and the absorption tower; h_{tower} is the height of the absorption tower; h_m is the height of the heliostat.

Constraint 2: Due to the movement of the absorption tower along the y-axis, taking the center of the base of the absorption tower as the origin (x_{q0}, y_{q0}), a Cartesian coordinate system is established. Thus, a point on the eccentric circle can be represented as $x_{qi}^2 + y_{qi}^2 = r_{qi}^2$. Convert the points on the eccentric circle into polar coordinate form based on the radius of the eccentric circle:

$$x_{qi} = r_{qi}\cos\theta_i, y_{qi} = r_{qi}\cos\theta_i \tag{12}$$

In order to reduce the effect of shadow obscuration, the heliostats on different layers are staggered, remembering that the positive direction of the y-axis on the horizon coordinate system is the starting rotation, the clockwise direction is the positive direction, and the coordinates of the heliostats on each layer are rotated clockwise by $q\lambda$, taken as $\lambda = 0.01rad$, which has the angle of the heliostat constraints:

$$x'_{qi} = r_{qi}\cos(\theta_i + q\lambda), y'_{qi} = r_{qi}\cos(\theta_i + q\lambda) \tag{13}$$

Constraint 3: The heliostat is shaped as a flat rectangle, with its top and bottom edges always parallel to the ground. The distance between these two edges is the height of the mirror surface, l_c, and the distance between the left and right edges of the mirror surface is its width, l_k . It is stipulated that all heliostats have the same dimensions and mounting height, h_m. Usually, the width of the mirror surface is not less than its height, and the length of the mirror edges ranges from 2m to 8m. Hence, there are constraints on the dimensions of the heliostat:

$$l_{ci} = l_{cj}, l_{ki} = l_{kj}, h_{mi} = h_{mj}, 2 \le l_c \le l_k \le 8 \tag{14}$$

Where: i and j are any two heliographs, and $1 \le i \le j \le N$.

Constraint 4: In order to ensure that the mirror will not touch the bottom surface when rotating around the horizontal rotary axis, the installation height should be greater than half of the width of the mirror, and the installation height is between 2m and 6m, which is recorded as the height constraint of the fixed-sun mirror:

$$h_m > l_k / 2, 2 \le h_m \le 6 \tag{15}$$

Constraint 5: The rated annual average output power of the heliostat field is 60 MW:

$$\sum_{month}^{12}\sum_{hour}^{5} E_{\text{field}} \ge 60MW \tag{16}$$

Constraint 6: Converting the points on the absorber tower coordinate system to the geodesic coordinate system, denoted as (x'_q, y'_q) , gives the coordinates of the absorber tower position as (x'_{q0}, y'_{q0}) , there:

$$x'_q = x_q, y'_q = y'_{q0} + y_q \tag{17}$$

Considering that the radius of the circular area of the heliostat field is 350m, and no heliostats are installed within a 100m range around the absorber tower, leaving open space for the construction of factory buildings for the installation of power generation, energy storage, control, and other equipment, there are boundary constraints for the heliostats:

$$x_q^2 + (y'_{q0} + y_q)^2 < 350^2, x_1^2 + y_1^2 \le (100 + \frac{l_k}{2})^2 \tag{18}$$

Constraint 7: Remember that there are two neighboring heliographs i , with coordinates $i+1$ (x_{qi}, y_{qi}) , (x_{qi+1}, y_{qi+1}) at the same q level and that the distance between the bases of the neighboring heliographs is $d_{qi-qi+1}$:

$$d_{qi-qi+1} = \sqrt{(x_{qi} - x_{qi+1})^2 + (y_{qi} - y_{qi+1})^2} \tag{19}$$

In order to facilitate the maintenance of the sun-setting mirror group and the need to clean the vehicle driving, the requirements of the distance between the center of the adjacent sun-setting mirror base is more than the mirror width of more than 5m, but also taking into account as much as possible

to improve the land utilization rate of the sun-setting mirror field to increase the reflective area, there is a sun-setting mirror spacing constraints:

$$d_{qi-qi+1} - \frac{l_{ki} + l_{ki+1}}{2} = 5 \tag{20}$$

Where: l_{ki} , l_{ki+1} denote the width of two neighboring heliographs on the same ring, respectively.

Due to the large number of decision variables and high computational space complexity, a simplified method is used to list the absorption tower position coordinates separately as the traversal object, on the basis of which the optimal solutions for the rest of the decision variables are searched with the help of genetic algorithms[10].The genetic algorithm based on the traversal strategy can finally be solved to obtain the annual average output thermal power per unit mirror area of the fixed-heaven mirror field.

According to the traversal situation, it can be seen that the maximum annual average output thermal power per unit mirror area is 0.5968kW/m^2, which is 20.8996% higher than the results of model I. At this time, the coordinates of the absorption tower are (0, -180) m, the dimensions of the heliostat mirror (width×height) are 7.5m×7.5m, and the height of the heliostat mirror installation is 4m.

The average optical efficiency and the average thermal power output per unit area mirror on the 21st day of each month kept changing with time, showing a trend of increasing and then decreasing, and the average thermal power output per unit area mirror in summer was higher than that in winter.

The annual average optical efficiency and output power are as shown in Table 2:

Table.2. The annual average optical efficiency and output power

annual average optical efficiency	annual average cosine efficiency	Average annual shadows Sheltering efficiency	annual average truncation efficiency	Average annual output Thermal power (MW)	Annual average of mirrors per unit area Output thermal power (KW/m)2
0.5881	0.8277	0.9537	0.8200	67.5331	0.5698

At this time, the average annual output thermal power of the fixed-sun mirror field is 67.5331kW/m^2, which reaches the rated power of 60MW, and the parameters of the fixed-sun mirror field at this time are as shown in Table 3:

Table.3. Annual design parameters of the heliostat field optimization model

Absorption tower position coordinates	Fixed Sun Mirror Size (W×H)	Installation height of fixed-sun mirror(m)	Total number of heliostats	Total area of the heliostat (m2)
(0, -180)	7.5 × 7.5	4	2107	118518.8

5. Conclusions

As a cutting-edge clean energy technology, tower-type solar thermal power generation holds the most promise in the current solar energy generation landscape. The overall research direction of this topic is the optimization design of the fixed sun mirror field. The article provides a comprehensive analysis of the working process of fixed sun mirrors, considering a variety of factors such as three types of shadow occlusion and spillage efficiency. By modeling the shadow occlusion efficiency, collector truncation efficiency, and optical efficiency of fixed sun mirrors, and optimizing some parameters of the fixed sun mirror field, the aim is to improve the annual average output thermal power per unit mirror surface area, providing assistance for theoretical research.

The model further takes into account multiple aspects such as performance, materials, structure, safety, and cost-effectiveness for designing and optimizing the solution. Moreover, based on field

surveys, it incorporates the impact of external environmental factors, considering the morphology of the fixed sun mirror field site, as well as engineering geology and hydrological conditions, thereby improving the annual average output thermal power per unit mirror surface area. In practical applications, it is possible to consider integration with other new energy sources for multi-energy integrated power generation, enhancing the energy storage efficiency of tower-type solar thermal power stations, and contributing to China's energy transformation and upgrade.

References

[1] Chang T P. The Sun's apparent position and the optimal tilt angle of a solar collector in the northern hemisphere[J]. Solar Energy, 2009, 83(8):1274-1284.

[2] Manish R, Jishnu B. An accurate and cheaper method of estimating shading and blocking losses in a heliostat field through efficient filtering, removal of double counting and parallel plane assumption[J]. Solar Energy,2022,243469-482.

[3] Bouamra M, Merzouk M. Cosine Efficiency Distribution with Reduced Tower Shadowing Effect in Rotating Heliostat Field[J]. Arabian Journal for Science and Engineering,2019,44(2):1415-1424.

[4] Zengqiang L, Xiaoxia L, Yuhong Z, et al.Determination of simulation parameters in Monte Carlo ray tracing for radiative flux density distribution simulation[J].Energy,2023,276

[5] Yang S, Lee K, Lee I. Pattern-free heliostat field layout optimization using physics-based gradient[J]. Solar Energy,2020,206722-731.

[6] Wang J, Duan L, Yang Y, et al.Rapid design of a heliostat field by analytic geometry methods and evaluation of maximum optical efficiency map[J].Solar Energy,2019,180456-467.

[7] Laporte-Azcué M, González-Gómez P, Rodríguez-Sánchez M, et al.Exergy analysis of solar central receivers[J].Solar Energy,2020,207957-973.

[8] Yu X, Manajit S, Jaemo Y, et al.Integration of a physics-based direct normal irradiance (DNI) model to enhance the National Solar Radiation Database (NSRDB)[J].Solar Energy,2023,266

[9] Wenjie W. The Explicit Expression of Axis and Angle of a Rotation Matrix[J]. The College Mathematics Journal,2021,52(1):39-44.

[10] Muhammad H, Ur A R, Sheeraz I, et al.Genetic algorithm optimization of heliostat field layout for the design of a central receiver solar thermal power plant[J].Heliyon,2023,9(11).